

EFFECT OF MICROSTRUCTURE ON MECHANICAL PROPERTIES IN FRICTION STIR WELDED CAST A356 ALUMINUM ALLOY

By Yutaka S. Sato*, Takayasu Kaneko, Mitsunori Urata and Hiroyuki Kokawa

Department of Materials Processing, Graduate School of Engineering, Tohoku University,
Aoba-yama 02, Sendai 980-8579, Japan, ytksato@material.tohoku.ac.jp

ABSTRACT

Friction stir welding (FSW) is a relatively new solid-state joining process which can homogenize the heterogeneous microstructure by intensely plastic deformation arising from the rotation of the welding tool. The present study applied the FSW to an A356 aluminum (Al) alloy with the as-cast heterogeneous microstructure in the T6 temper condition, and examined an effect of microstructure on mechanical properties in the weld. The base material consisted of Al matrix with a high density of strengthening precipitates, large eutectic silicon and a lot of porosities. The FSW led to fragment of the eutectic silicon, extinction of the porosities and dissolution of the strengthening precipitates in the Al alloy. The dissolution of strengthening precipitates reduced the hardness of the weld around the weld center and the transverse ultimate tensile strength of the weld. Longitudinal tensile specimen containing only the stir zone showed the roughly same strength as the base material and a much larger elongation. Moreover, Charpy impact tests indicated that the stir zone had remarkably the higher absorbed energy than the base material. The higher mechanical properties of the stir zone were attributed to a homogenization of the as-cast heterogeneous microstructure by FSW.

KEYWORDS

Friction stir welding, cast aluminum alloy, microstructure, mechanical properties, precipitation

1. Introduction

The hypoeutectic alloys in the Al-Si-Mg system have a wide range of applications in the aerospace and automotive industries[1,2]. The entire Al-Si-Mg alloys have excellent casting characteristics and corrosion resistance. The minor addition of Mg in Al-Si-Mg alloys combines with Si to form the strengthening precipitates during T6 heat treatment (solution heat treatment following aging)[3], which results in the higher mechanical properties in the alloys. The A356 Al alloy is one of the most common cast Al alloys in the Al-Si-Mg system.

When the cast Al alloys are in a practical use, welding and joining procedures are often required. However, conventional fusion-welding processes for the cast Al alloy are generally difficult because many porosities existing in the base material are often entrapped in the fusion zone during solidification of fusion-welding process[4]. Moreover, solute elements, especially Mg, vaporize from molten metal, which reduces mechanical properties of fusion zone[1].

Much attention has been directed recently to FSW for Al alloys[5]. The FSW makes the weld in solid phase by locally introducing frictional heating and intensely plastic deformation arising from rotation of the welding tool, leading to fine recrystallized grains in the stir zone[6-33]. This feature suggests that the FSW can produce a high-quality, defect-free weld in cast Al alloy more easily than fusion welding process. Moreover, the cast Al alloys generally have the as-cast heterogeneous microstructure, which results in a low ductility in the alloys. Some studies[8,22,34] reported that the FSW homogenized the heterogeneous microstructure produced by casting or powder metallurgy, so that the homogenization of the as-cast microstructure by FSW probably improves the mechanical properties. However, there are few previously reported papers on the FSW for cast Al alloys. The present study examined the microstructural distribution and several mechanical properties in friction stir (FS) weld of cast A356 Al alloy. The objective of the present study is to clarify relationship between mechanical properties and microstructure in the weld.

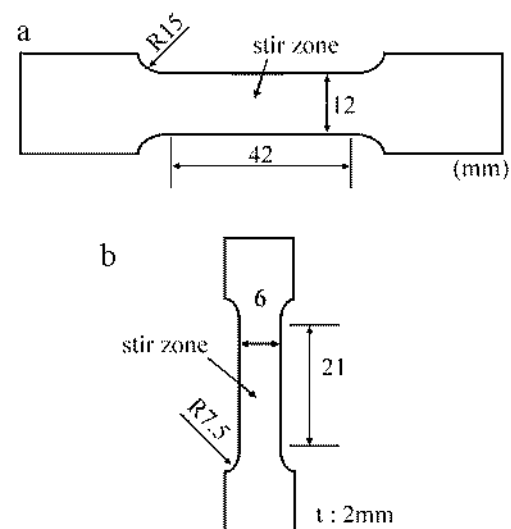


Fig. 1 Configurations of transverse tensile specimen (a) and longitudinal tensile specimen (b).

2. Experimental Procedures

The base material used in the present study was an as-cast A356 Al alloy in T6 temper condition, 4 mm in thickness. Its chemical composition was Al-9.23Si-0.36Fe-0.09Cu-0.60Mn-0.45Mg-0.03Cr-0.08Zn-0.03Ti (all compositions are in wt-%). The base material plate was FS-welded at rotation speed of 1220 rpm and traveling speed of about 5.9 mm/s.

Vickers hardness profile, tensile properties and absorbed energy by Charpy impact test were examined with the weld. Hardness profile was measured on cross section perpendicular to the welding direction. Tensile specimens were cut from the weld using an electrical-discharge machine. Configurations of the tensile specimens are shown in Fig. 1. Transverse specimen (Fig 1(a)) and longitudinal specimen (Fig.1(b)) were cut perpendicular and parallel to the welding direction, respectively. The gauge part of the transverse specimen extended from the stir zone to the base-material region, while the longitudinal specimen contained only the stir zone in the gauge part. Tensile tests were carried out at room temperature on a screw-driven test machine at a cross-head speed of 1.67×10^{-2} mm/s. Charpy impact tests were applied to the base material and the weld having the notch in the center of the stir zone at the temperatures of 77, 273 and 333 K.

Variation in microstructure was examined by optical microscopy, scanning electron microscopy (SEM) and transmission electron microscopy (TEM). Eutectic silicon was observed by optical microscopy and SEM. Compositions of eutectic silicon were analyzed by a HITACHI S4700 SEM equipped with an energy-dispersive X-ray spectroscopy (EDS) analysis system. Grain structures of the base material and heat-affected zone (HAZ) were observed in the specimen anodized in Barker's solution under the polarized light, while that of the stir zone was drawn by orientation imaging microscopy (OIM). The precipitate distribution in the weld was observed by TEM. Thin disks for TEM observation, which were cut from various locations in the weld using an electrical-discharge machine, were prepared using the procedure of grinding, dimpling and ion milling. The TEM observation was carried out in a JEOL 2000EXII instrument operating at 200 kV. The incident electron beam was controlled to a $\langle 100 \rangle$ zone axis of the matrix in all the bright-field images.

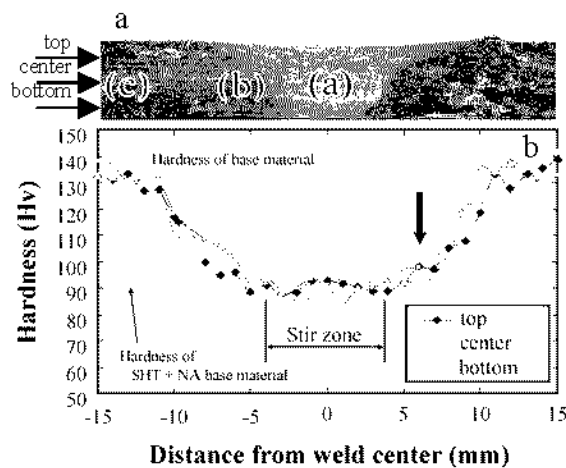


Fig. 2 Cross section perpendicular to the welding direction (a) and hardness profiles across the stir zone (b).

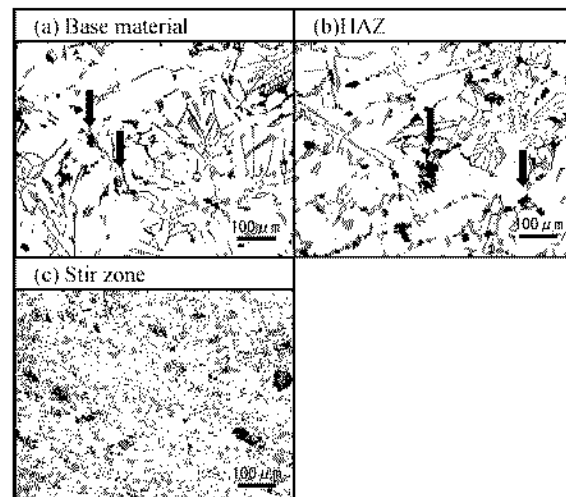


Fig. 3 Optical microstructures at locations "a," "b," and "c," shown in Fig. 2(a).

3. Results and Discussion

Low-magnification overview of FS-welded cast A356 Al alloy is shown in Fig. 2(a). The base-material region has a number of large porosities. The stir zone, that is observed around the weld center, exhibits a high degree of continuity and no porosity. The stir zone widens near the upper surface.

Hardness profiles across the stir zone in the weld are indicated in Fig. 2(b). The notations of "top," "center" and "bottom" are shown by three arrows in Fig. 2(a). The average hardness values of the as-received T6 base material and the solution-heat-treated and natural aged (SHT + NA) base materials are also added by dotted lines in this figure. The T6 base material has an average hardness value of about 136 Hv, but the FSW reduces the hardness to that of the SHT + NA base material around the weld center. The softening spreads from the stir zone to heat-affected zone (HAZ). Almost no difference is observed in hardness profiles among top, center and bottom lines.

Figure 3 shows optical microstructures at locations "a," "b," and "c," shown in Fig. 2(a). Regions "a" through "c" correspond to "the unaffected base-material region," "the HAZ," and "the stir zone", respectively. The base-material region has the as-cast heterogeneous microstructure consisting of the Al matrix and large eutectic

silicon. Many porosities are distributed in the as-cast microstructure, as shown by arrows in Fig. 3. The HAZ shows the roughly same microstructure as the base-material region. On the other hand, the stir zone has the very fine eutectic silicon and no porosities.

Composition analysis by EDS indicated that there was almost no difference in composition of eutectic silicon among all regions. No significant difference in the composition among all regions means that the large eutectic silicon fragments during the stirring of FSW and disperse in the stir zone. The extinction of porosities in the stir zone is due to the intense plastic deformation during FSW. It is possible that the hardness profile in the weld depends on morphology and size of eutectic silicon. A previous study[2] has shown that size of eutectic silicon hardly affect hardness value in cast Al-Si alloys. This report suggests that hardness profile depends on the other microstructural factors in the weld of cast A356 Al alloy.

In order to examine grain size profile in the weld, the weld was anodized by Barker's solution. This gives a grain-orientation contrast when viewed under polarized light. The examination showed that the base-material region and the HAZ had the average grain sizes of 537 and 522 μm , respectively. On the other hand, grain-orientation contrast could not be distinguished in the stir zone. The grain size of the stir zone was obtained using OIM image drawing grain boundaries with misorientation angle of 15 degrees. The average grain size in the stir zone was 5.31 μm , which was much smaller than grain sizes of the base-material region and the HAZ. Generally, the finer grain size raises the strength and hardness of the metallic material through the Hall-Petch equation, but the grain size profile is not consistent with the hardness profile in the weld. Cast A356 Al alloy used in the present study is a typical precipitation-hardenable alloy. In the precipitation-hardenable Al alloy, the hardness depends strongly on the precipitate distributions rather than on grain size, as stated in previous studies [6,7,9,11-13,17,19,27,29,31]. This suggests that the hardness profile cannot be explained by grain size, but by precipitate distributions in the weld.

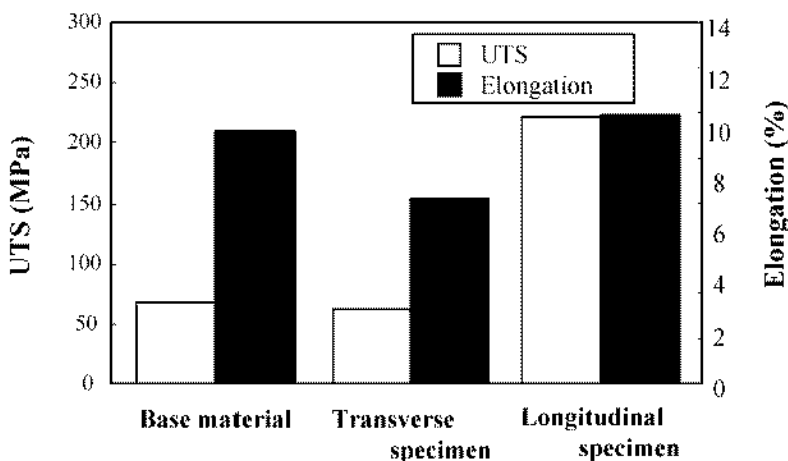


Fig. 5 Tensile properties of the base material, transverse specimen and longitudinal specimen.

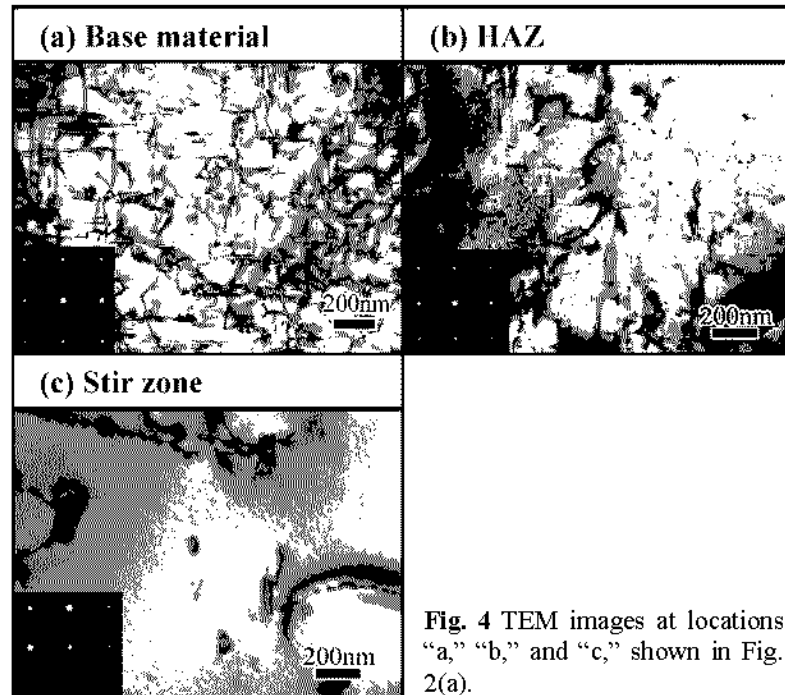


Fig. 4 TEM images at locations "a," "b," and "c," shown in Fig. 2(a).

TEM images obtained from Al matrices of the base-material region, the HAZ and the stir zone are indicated in Fig. 4. The base-material region has a high density of fine needle-shaped precipitates. The density of needle-shaped precipitates is reduced in the HAZ, and the needle-shaped precipitates cannot be observed in the stir zone. It is generally known that a high density of needle-shaped precipitates formed by Mg and Si contributes to the strength of A356 Al alloy in the T6 temper condition[2]. This result reveals that the density of

needle-shaped precipitates in Al matrix can explain the hardness profile in the weld. The decrease in the density of the precipitates is due to the dissolution of needle-shaped precipitates during FSW.

Tensile properties of the base material, transverse and longitudinal specimens are summarized in Fig. 5. The base material has a relatively high ultimate tensile strength (UTS) and a low elongation. Transverse tensile specimen of the weld experiences a remarkable decrease in UTS and a slight decrease in elongation. Fracture of the transverse specimen occurred in the HAZ shown by arrow in Fig. 2(b). On the other hand, longitudinal tensile specimen of the weld has the roughly same UTS as the base material and the much larger elongation. Stress-strain curves showed that the base material and the transverse specimen fractured during elastic deformation, while fracture of the longitudinal specimen occurred during plastic deformation before plastic instability.

The base material and the transverse specimen showed the low elongation. This is because that both the base material and the HAZ consist of the as-cast heterogeneous microstructure and many porosities. The lower UTS of the transverse specimen than the base material can be explained by the lower hardness values in the HAZ, because the transverse specimen of the weld with heterogeneous hardness profile fractured at the minimum hardness region during tensile test and the minimum hardness determined the global tensile strength of the transverse specimen[27]. The higher elongation in the longitudinal specimen is attributed to the stir zone with fine recrystallized microstructure containing both wide dispersion of fine eutectic silicon and no porosities. Since the hardness value is proportional to the yield strength in the general material[35], the longitudinal specimen should show the lower strength than the base material. However, both the base material and the HAZ contain many porosities, as shown in Fig. 3. It is possible that the presence of the porosity results in stress concentration at the porosity during tensile test. The stress concentration probably leads to a fracture at the stress lower than the UTS. Fractographs of the base material, transverse and longitudinal specimens, that are indicated in Fig. 6, show that many porosities are observed in fracture surfaces of the broken base-material specimen and transverse specimen. These results suggest that the stress concentration at the porosity is a possible reason for the roughly same UTS of the longitudinal specimen as the base material.

Results of the Charpy impact test for the base material and the stir zone are presented in Fig. 7. The absorbed energy of the base material is very low at the temperature range of 77 to 333 K, while the stir zone shows the significantly higher absorbed energy than the base material. The absorbed energies of the base material and the stir zone slightly increase with increasing the test temperature. The FSW produces the fine recrystallized grain structure with wide dispersion of fine eutectic silicon and no porosities in the stir zone. Such microstructure causes the higher absorbed energy of the stir zone.

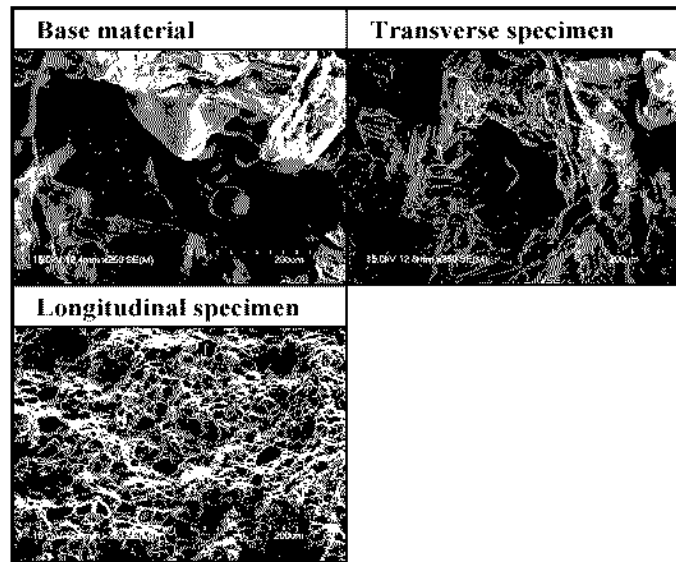


Fig. 6 Fractographs of the base material, transverse specimen and longitudinal specimen after tensile tests.

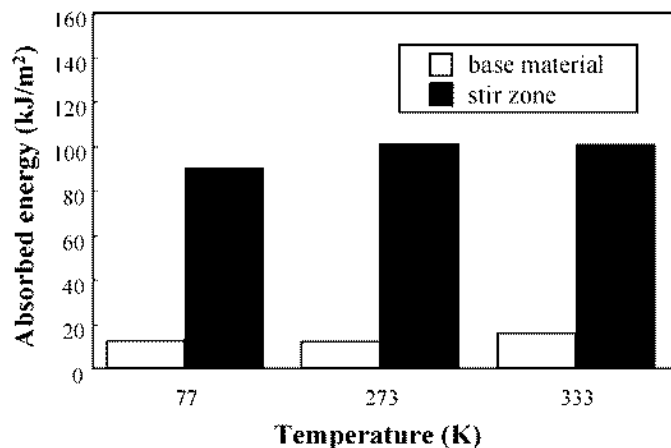


Fig. 7 Absorbed energies of the base material and the stir zone at temperatures of 77, 273 and 333 K.

4. Conclusions

The present study applied the FSW to cast A356 Al alloys in the T6 temper condition, and examined the relationship between mechanical properties and microstructure in the weld. The base material had the as-cast heterogeneous microstructure having large eutectic silicon and many porosities, while the FSW produced the stir zone with fine recrystallized grain structure containing both wide dispersion of fine eutectic silicon and no porosities. The hardness of the weld was reduced around the weld center. The transverse tensile specimen fractured in the HAZ and had a lower UTS than the base material. The dissolution of the strengthening precipitates reduced the hardness around the weld center and the UTS of the transverse tensile specimen of the weld. The longitudinal tensile specimen containing only the stir zone showed the roughly same strength as the base material and a significantly larger elongation. Moreover, Charpy impact tests indicated that the stir zone has remarkably the higher absorbed energy than the base material. The higher mechanical properties of the stir zone were attributed to a homogenization of the as-cast heterogeneous microstructure by FSW.

Acknowledgements

The authors are grateful to Mr. A. Honda for technical assistance. They thank Dr. M. Enomoto, Mr. S. Jogan, Dr. T. Hashimoto, Dr. T. Kanai and Mr. S. Sato for useful advice. They are also grateful to Prof. K. Ikeda, Prof. Z.J. Wang and Mr. S.H.C. Park for the helpful discussion. Financial support from the Japanese Ministry of Education, Science, Sports and Culture with a Grant-in-Aid for Encouragements of Young Research is gratefully acknowledged.

References

- [1] L.-R. Hwang, C.-H. Gung and T.-S. Shih: *J. Mater. Process. Technol.*, 116(2001), p.101.
- [2] S. Kitaoka, C. Fujikura and A. Kamio: *J. Jpn Inst. Light Met.*, 37(1988), p.426.
- [3] M. Koga, N. Ohnishi, Y. Iizuka, T. Takaai and Y. Nakayama: *J. Jpn Inst. Light Met.*, 43(1993), p.297.
- [4] T. Okita: *J. Light Met. Welding Construction*, 39(2001), p.449.
- [5] C.J. Dawes and W.M. Thomas: *Weld. J.*, 75(1996), March, p.41.
- [6] C.G. Rhodes, M.W. Mahoney, W.H. Bingel, R.A. Spurling, C.C. Bampton: *Scripta Mater.*, 36(1997), p.69.
- [7] G. Liu, L.E. Murr, C.-S. Niou, J.C. McClure and F.R. Vega: *Scripta Mater.*, 37(1997), p.355.
- [8] L.E. Murr, G. Liu and J.C. McClure: *J. Mater. Sci. Lett.*, 16(1997), p.1801.
- [9] L.E. Murr, G. Liu and J.C. McClure: *J. Mater. Sci.*, 33(1998), p.1243.
- [10] O.V. Flores, C. Kennedy, L.E. Murr, D. Brown, S. Pappu, B.M. Nowak and J.C. McClure: *Scripta Mater.*, 38(1998), p.703.
- [11] M.W. Mahoney, C.G. Rhodes, J.G. Flintoff, R.A. Spurling and W.H. Bingel: *Metall. Mater. Trans.*, 29A(1998), p.1955.
- [12] Y.S. Sato, H. Kokawa, M. Enomoto and S. Jogan: *Metall. Mater. Trans.*, 30A(1999), p.2429.
- [13] Y.S. Sato, H. Kokawa, M. Enomoto, S. Jogan and T. Hashimoto: *Metall. Mater. Trans.*, 30A(1999), p.3125.
- [14] Y. Li, L.E. Murr and J.C. McClure: *Mater. Sci. Eng.*, A271(1999), p.213.
- [15] S. Benavides, Y. Li, L.E. Murr, D. Brown and J.C. McClure: *Scripta Mater.*, 41(1999), p.809.
- [16] R.S. Mishra, M.W. Mahoney, S.X. McFadden, N.A. Mara and A.K. Mukherjee: *Scripta Mater.*, 42(2000), p.168.
- [17] K.V. Jata, K.K. Sankaran and J.J. Ruschau: *Metall. Mater. Trans.*, 31A(2000), p.2181.
- [18] K.V. Jata and S.L. Semiatin: *Scripta Mater.*, 43(2000), p.743.
- [19] L.-E. Svensson, L. Karlsson, H. Larsson, B. Karlsson, M. Fazzini and J. Karlsson: *Sci. Technol. Weld. Joining*, 5(2000), p.285.
- [20] Y. Li, E.A. Trillo and L.E. Murr: *J. Mater. Sci. Lett.*, 19(2000), p.1047.
- [21] J. Corral, E.A. Trillo, Y. Li and L.E. Murr: *J. Mater. Sci. Lett.*, 19(2000), p.2117.
- [22] P.B. Berbon, W.H. Bingel, R.S. Mishra, C.C. Bampton and M.W. Mahoney: *Scripta Mater.*, 44(2001), p.61.
- [23] Y.S. Sato, H. Kokawa, K. Ikeda, M. Enomoto, S. Jogan and T. Hashimoto: *Metall. Mater. Trans.*, 32A(2001), p.941.
- [24] Y.S. Sato, M. Urata, H. Kokawa, K. Ikeda and M. Enomoto: *Scripta Mater.*, 45(2001), p.109.
- [25] N. Saito, I. Shigematsu, T. Komaya, T. Tamaki, G. Yamauchi and M. Nakamura: *J. Mater. Sci. Lett.*, 20(2001), p.1913.
- [26] D.P. Field, T.W. Nelson, Y. Hovanski and K.V. Jata: *Metall. Mater. Trans.*, 32A(2001), p.2869.
- [27] Y.S. Sato and H. Kokawa: *Metall. Mater. Trans.*, 32A(2001), p.3023.
- [28] Y.S. Sato, S.H.C. Park and H. Kokawa: *Metall. Mater. Trans.*, 32A(2001), p.3033.
- [29] Y.S. Sato, M. Urata, H. Kokawa, K. Ikeda and M. Enomoto: *Proc. of the 7th Int. Symp.*, JWS, Kobe, (2001), p.633.
- [30] H. Jin, S. Saimoto, M. Ball and P.L. Threadgill: *Mater. Sci. Technol.*, 17(2001), p.1605.
- [31] Y.S. Sato, M. Urata and H. Kokawa: *Metall. Mater. Trans.*, 33A(2002), p.625.
- [32] M.A. Sutton, B. Yang, A.P. Reynolds and R. Taylor: *Mater. Sci. Eng.*, A323(2002), p.160.

- [33] Y.S. Sato, M. Urata, H. Kokawa, K. Ikeda and M. Enomoto: *Proc. of the 6th Int. Conf. Trends in Weld. Res.*, ASM International, Pine Mountain, (2002), in press.
- [34] M.B.D. Ellis and M. Stranwood: *Mater. Sci. Technol.*, 12(1996), p.970.
- [35] M.F. Ashby and D.R.H. Jones: *Engineering Materials 1*, Pergamon Press, Oxford, UK, 1980, p.105.